Pergamon

Geochimica et Cosmochimica Acta, Vol. 67, No. 22, pp. 4223–4230, 2003

0016-7037/03 $30.00 + .00

doi:10.1016/S0016-7037(03)00237-0

Surface complexation of arsenic(V) to iron(III) (hydr)oxides: Structural mechanism from ab initio molecular geometries and EXAFS spectroscopy

DAVID M. SHERMAN* and SIMON R. RANDALL
Department of Earth Sciences, University of Bristol, Bristol BS8 1RJ, UK

(*Received November* 12, 2002; *accepted in revised form March* 20, 2003)

Abstract—Arsenic(V), as the arsenate $(AsO_4)^{3-}$ ion and its conjugate acids, is strongly sorbed to iron(III) oxides (α-Fe_2O_3), oxide hydroxides (α–,γ–FeOOH) and poorly crystalline ferrihydrite (hydrous ferric oxide). The mechanism by which arsenate complexes with iron oxide hydroxide surfaces is not fully understood. There is clear evidence for inner sphere complexation but the nature of the surface complexes is controversial. Possible surface complexes between AsO_4 tetrahedra and surface FeO_6 polyhedra include bidentate corner-sharing (^{2}C), bidentate edge-sharing (^{2}E) and monodentate corner-sharing (^{1}V). We predicted the relative energies and geometries of AsO_4-FeOOH surface complexes using density functional theory calculations on analogue $Fe_2(OH)_2(H_2O)_nAsO_2(OH)_2^{3+}$ and $Fe_2(OH)_2(H_2O)_nAsO_4^{+}$ clusters. The bidentate corner-sharing complex is predicted to be substantially (55 kJ/mole) more favored energetically over the hypothetical edge-sharing bidentate complex. The monodentate corner-sharing (^{1}V) complex is very unstable. We measured EXAFS spectra of 0.3 wt. % $(AsO_4)^{3-}$ sorbed to hematite (α-Fe_2O_3), goethite(α–FeOOH), lepidocrocite(γ–FeOOH) and ferrihydrite and fit the EXAFS directly with multiple scattering. The phase-shift-corrected Fourier transforms of the EXAFS spectra show peaks near 2.85 and 3.26 Å that have been attributed by previous investigators to result from ^{2}E and ^{2}C complexes. However, we show that the peak near 2.85 Å appears to result from As-O-O-As multiple scattering and not from As-Fe backscatter. The observed 3.26 Å As-Fe distance agrees with that predicted for the bidentate corner-sharing surface (^{2}C) complex. We find no evidence for monodentate (^{1}V) complexes; this agrees with the predicted high energies of such complexes. *Copyright © 2003 Elsevier Ltd*

1. INTRODUCTION

Under moderately acidic conditions, arsenic(V) as $H_nAsO_4^{3-n}$ is strongly sorbed by iron oxides and oxide hydroxides such as ferrihydrite, goethite and hematite (Fuller et al., 1993; Waychunas et al., 1993; Sun and Doner, 1996; Jain et al., 1999). The strong sorption of As onto these minerals is invoked as an important mechanism of natural attenuation of As pollution in soil and groundwater (Livesey and Huang, 1981) and lacustrine sediments (Aggett and Roberts, 1986; Belzile and Tessier, 1990). Sorption onto iron oxide hydroxide minerals is especially significant in controlling As solubilities in acid mine drainage and mine-tailings ponds (Carlson et al., 2002). The marine geochemistry of arsenic also indicates control by sorption onto iron oxide hydroxides (Sullivan and Aller, 1996; Pichler et al., 1999).

A molecular understanding of the sorption of arsenic by iron oxides and oxyhydroxides is needed to predict the long-term fate of As in aqueous sediments. Previous spectroscopic studies (e.g., Waychunas et al., 1993, 1995; Hsia et al., 1994; Sun and Doner, 1996; Fendorf et al., 1997), pressure-jump relaxation kinetics measurements (Grossl and Sparks, 1995; Grossl et al., 1997) and titration measurements (Jain et al., 1999) show that arsenate adsorbs to iron oxide hydroxides by forming inner-sphere surface complexes by ligand exchange with hydroxyl groups at the mineral surface. However, the nature of the inner-sphere complex has been controversial (Fig. 1). Using EXAFS spectroscopy, Waychunas et al. (1993) argued for bidentate complexes (^{2}C in Fig. 1) resulting from corner-sharing between AsO_4 tetrahedra and edge-sharing pairs of FeO6 octahedra. The ^{2}C complex yields an As-Fe distance near 3.26 Å. For goethite (α-FeOOH), the ^{2}C complex would form on the {110} surfaces which are, in fact, the dominant surfaces (e.g., Boily et al., 2001). Waychunas et al. (1993) also fit their data to a second contribution corresponding to monodentate complexes (designated ^{1}V in Fig. 1) that result from corner-sharing between AsO_4 tetrahedra and FeO_6 octahedra. The ^{1}V complex gives an As-Fe distance near 3.6 Å. Manceau (1995), however, argued that Waychunas et al. (1993) incorrectly calculated the phase shifts in the EXAFS spectra and that the correct As-Fe distance for the second complex is near 2.8 Å; such a short As-Fe distance would result from bidentate edge-sharing between AsO_4 tetrahedra and free FeO_6 edges (designated ^{2}E in Fig. 1). In goethite, the 2E complex would form on

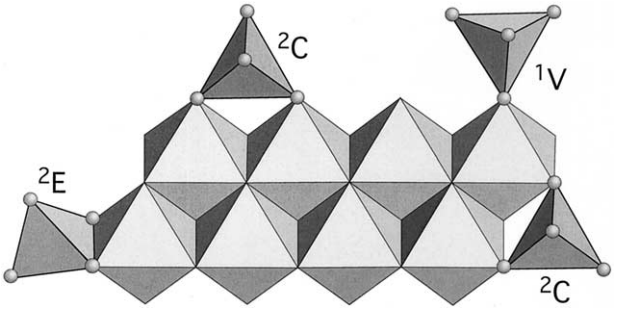

Fig. 1. Possible surface complexes of AsO_4 tetrahedra on goethite.

* Author to whom correspondence should be addressed (dave.sherman@bris.ac.uk).

the {001} and {021} faces which usually comprise a small fraction of the goethite surface (e.g., Boily et al., 2001). Waychunas et al. (1995, 1996) argued against the ^{2}E complex for structural reasons, problems with fits of EXAFS that include a ^{2}E complex, and wide-angle scattering data that fail to show any distance corresponding to a ^{2}E complex.

Fendorf et al. (1997) interpreted their EXAFS data as indicating three surface complexes: a monodentate corner sharing (^{1}V) complex with an As-Fe distance of 3.6 Å, a bidentate corner-sharing (^{2}C) with two As-Fe distances near 3.25 Å and a bidentate edge-sharing complex (^{2}E) with a single As-Fe distance of 2.83–2.85 Å. Fendorf et al. (1997) proposed that the relative importance of each complex depended on the degree of surface loading. Farquhar et al. (2002) obtained EXAFS of As(V) on goethite and lepidocrocite and found peaks in the Fourier transform near 2.93 Å and 3.30–3.31 Å. They attributed the 3.30–3.31 Å peaks to (^{2}C) complexes but were uncertain if the 2.93 Å peak represented a ^{2}E complex.

In this paper, we attempt to resolve the controversy over the inner-sphere surface complexation mechanism: we first predict the geometries and relative energies of AsO_4-FeOOH surface complexes using density functional theory calculations on analog $Fe_2(OH)_2(H_2O)_nAsO_4^{+}$ and $Fe_2(OH)_2(H_2O)_nAsO_2(OH)_2^{+3}$ clusters. Secondly, we measure EXAFS spectra of AsO_4 sorbed to goethite, hematite, lepidocrocite and ferrihydrite but fit the data with inclusion of effects due to multiple scattering. From these results, we are able to identify the dominant surface complex of AsO_4 on iron oxides and oxide hydroxide phases and are also able to explain discrepancies between earlier experimental results.

2. EXPERIMENTAL AND COMPUTATIONAL METHODS

2.1. Density Functional Calculations

Quantum mechanical calculation of cluster geometries and energies were done using the ADF 2.0 code (te Velde et al., 2001) which implements density functional theory for finite clusters and molecules using the linear combination of atomic orbital formalism. Molecular orbitals in the ADF code are constructed from Slater type atomic orbitals which consist of a Cartesian part $r^{kr}x^{kx}y^{ky}z^{kz}$ with $k_x+k_y+k_z = l$ (l = angular momentum quantum number) and an exponential part $e^{-\alpha r}$. Density functional theory allows very large basis set to be used: For all atoms, we used an uncontracted, triple-zeta basis set with polarization functions (i.e., 1s2s2p3s3p3d3d′3d′′ 4s4s′4s′′+4p for iron, 1s2s2s′2s′′+3d for oxygen, 1s2s2p3s3p3d3d′3d′′4s4s′4s′′4p4p′4p′′ +3d for arsenic and 1s1s′1s′′+2p for hydrogen). The charge density was also fit to a Slater type orbital basis set. For all atoms except hydrogen, we used frozen core orbitals (i.e., 1s, 2s, 2p and 3p for Fe; 1s for O and 1s, 2s, 2p and 3p for As).

We used the Vosko et al. (1980) parameterization for the local exchange-correlation functionals together with generalized gradient corrections of Perdew et al. (1992). All calculations were done using the spin-unrestricted formalism.

The geometries of the clusters were optimized using a Newton-Raphson method and Broydon-Fletcher update of the Hessian matrix as coded in ADF 2.0. During the geometry optimizations the total energies were converged to +/− 5 kJ/mole. We allowed all atomic coordinates to vary in an attempt to simulate the surface relaxation of bond lengths and angles.

2.2. Synthesis of As-FeOOH, As-Fe_2O_3 and As-Ferrihydrite Complexes

All reagents used in this study were analytical grade and labware was acid-washed. pH measurements were calibrated to ± 0.05 pH units using Whatman NBS grade buffers. The As(V) stock solution was prepared from $Na_2HAsO_4 \cdot 7H_2O$ and was stored at 4 °C in a closed amber-coloured HDPE bottle. Plastic labware was used at high pH to avoid the danger of leaching silica from glassware.

2.2.1. Preparation of As sorbed on synthetic goethite, lepidocrocite and hematite

Goethite was prepared by hydrolyzing a ferric nitrate solution at pH 12–13 and 70 °C for 60 h (Schwertmann and Cornell, 1991). The crystal morphology was examined by TEM and electron diffraction. Goethite crystallites measured approximately 4000 nm long by 150 nm wide. They displayed a characteristic elongate lath-like morphology with a diamond shaped cross-section bounded mainly by the (110) surfaces with little or no contribution from the (100) and (010) surfaces. The chain terminations were bounded by the (021) surfaces which are estimated to comprise ~2% of the overall crystal surface area. The surface area of the synthesized goethite was measured by BET to be 34 ± 3 m^2 g^{-1}.

Hematite was prepared by hydrolysis of ferric nitrate at pH= 2.7 and 98 °C for 7 d (Schwertmann and Cornell, 1991). The product was characterized by X-ray diffraction and its surface area was determined to be 20 ± 3 m^2 g^{-1} using BET.

Lepidocrocite was prepared by the oxidation/hydrolysis of a ferrous chloride solution at pH 6.7 – 6.9 (Schwertmann and Cornell, 1991). The bright orange precipitate was collected by centrifugation, cleaned by dialysis against MilliQ water and stored as a refrigerated 20 g L^{-1} stock suspension before use. X-ray powder diffraction of a randomly oriented powder sample was used to confirm the identity and purity of the crystalline product. Additionally, its surface area (88 ± 3 m^2g^{-1}) was determined by BET surface area analysis following 12 h of outgassing with N_2(g). Transmission electron microscopy showed the crystallites to measure approximately 300 nm long by 120 nm wide and displayed the platy morphology that is characteristic of γ-FeOOH.

Suspensions of goethite, hematite and lepidocrocite were made by adding 0.5 g of each phase to 370 mL of 0.1m $NaClO_4$ and dispersing ultrasonically. Goethite and hematite were equilibrated with 4.0 and 3.36 ppm As at pH 3.9 ± 0.05 under ambient temperature and atmospheric conditions for 24 h. The lepidocrocite suspension was equilibrated with 4.0 ppm As at pH=7.0. Each suspension was then separated by centrifugation (3000 rpm for 20 – 60 min) into a clear supernatant and a viscous paste (the 'adsorption sample') which was frozen before analysis. The supernates were filtered using 0.2 μm cellulose nitrate membrane filters and analyzed for arsenic within 24 h of collection on a Jobin-Yvon JY-24 ICP-AES. Determinations of aqueous arsenic concentration by this technique are often reported to involve a hydride generation step. This was

not deemed necessary here as a pilot study showed that our ICP-AES was capable of returning accurate and repeatable determinations of arsenic concentration from a range of standards. The final molar As/Fe ratios of the samples are 0.0028, 0.0031, 0.0028 for goethite, hematite and lepidocrocite, respectively.

2.2.2. Preparation of As adsorbed and coprecipitated with ferrihydrite

Ferrihydrite was prepared by neutralizing a 0.2 mol/L ferric nitrate solution with 1M KOH according to the method reported by Schwertmann and Cornell (1991). The resulting deep brown slurry was rinsed clean of contaminant anions (e.g., NO_3^-) by repeated centrifugation and re-suspension in fresh MilliQ water. The clean suspension was allowed to age for 24 h at room temperature before being used. We equilibrated 5 g ferrihydrite with 1000 mL of 12.4 ppm As in 0.1 $NaClO_4$ electrolyte at pH 4 for two hours. Wilkie and Hering (1996) have previously established that this is long enough for the removal of 100% of available As(V) from solution between pH 4 and 8. Ferrihydrite samples were separated and analyzed as discussed above for the crystalline phases. For the first ferrihydrite sample, the final As/Fe = 0.0033. A second 5 g ferrihydrite sample was equilibrated in 1000 mL of 62.5 ppm As for 211 h to give a final As/Fe ratio of 0.016. X-ray diffraction of this sample showed no detectable crystalline phases present after 211 h.

A third ferrihydrite sample was prepared by coprecipitating Fe and As. Here, 40.0 g of ferric nitrate was hydrolyzed in 1000 mL of a 0.04 ppm As solution at pH = 4.0 to give a final As/Fe of 0.0054. X-ray diffraction analysis of the sample showed no detectable crystalline phases.

2.3. EXAFS Data Collection and Analysis

2.3.1. Data collection

EXAFS data were collected at the CLRC Synchrotron Radiation Source at Daresbury Laboratory, U.K. Spectra were collected at the arsenic K-edge (11.8667 keV) on station 16.5. Station 16.5 is equipped with a 1.2 m long plane mirror which is bent to provide vertical focusing. Because the focusing mirror minimized higher harmonics in the EXAFS spectra, it was not necessary to detune the monochromotor during data collection. This gave us a high flux allowing measurements on dilute samples. The storage ring energy was 2.0 GeV and the beam current varied between 130 and 240 mA during data collection. Each iron (hydr)oxide sample was mounted as a wet-paste held by Sellotape in a 2 mm-thick Teflon slide with a 4 × 15 mm sample slot. EXAFS data were collected from the samples by adding four to six fluorescence mode scans using an Ortec 30-element solid state detector. Data were collected for samples at room temperature. EXAFS data were also collected of scorodite ($FeAsO_4 \cdot 4H_2O$) in three room-temperature transmission mode scans.

2.3.2. EXAFS data analysis

EXAFS data reduction was performed using Daresbury Laboratory software EXCALIB and EXBACK (Dent and Mosselmans, 1992). EXCALIB was used to calibrate from monochromotor position (millidegrees) to energy (eV) and to average multiple spectra from individual samples. EXBACK was used to define the start of the EXAFS oscillations and perform background subtraction.

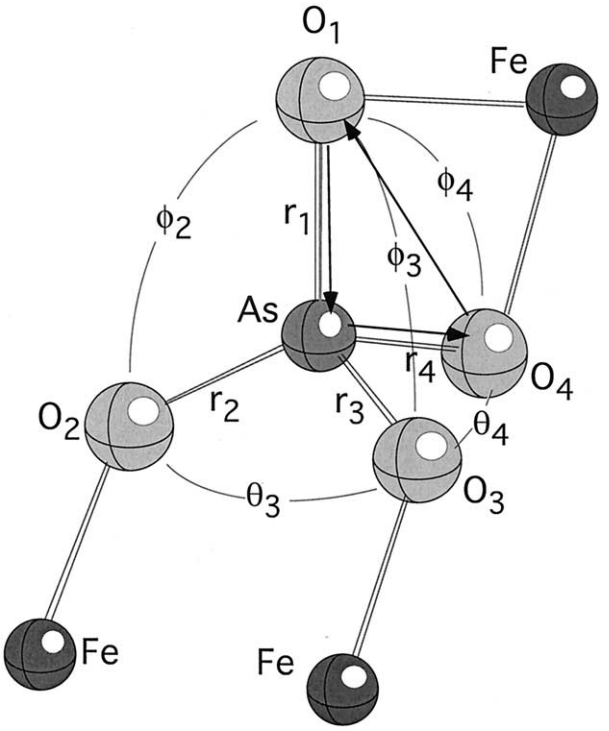

Fig. 2. Cluster used to model single- and multiple-scattering for EXAFS analysis. The bond angles were relaxed during the fits but showed little change from their ideal tetrahedral values of $\theta = 120°$ and $\phi = 109.5°$. The dominant multiple scattering path is shown by the arrows. Multiple scattering involving iron atoms was not significant.

It is important to note that we fit the EXAFS spectra directly and not the Fourier transform of the EXAFS (radial distribution function). To do this, we used the EXAFS analysis program EXCURV98 (Binsted, 1998) in the small-atom approximation and allowed for multiple scattering. Multiple scattering paths were limited to those involving 3 atoms. Longer paths had no obvious effect. The phase-shifts and potentials used in the fitting were derived by ab initio density functional calculations in EXCURV98 using Hedin-Lundqvist exchange-correlation functionals (Hedin and Lundqvist, 1969). The theoretical phase shifts were tested by comparing the bond lengths in scorodite obtained from our EXAFS data with those known from the crystal structure (Kitahama et al., 1975). The inclusion of multiple scattering (Gurman et al., 1986) was found to improve the fit in the 2.8–3.3 Å region where we found that some of the features result from O-O scattering within the AsO_4 tetrahedra. Multiple scattering calculations require specifying the full three dimensional structure of the As coordination environment (i.e., bond angles in addition to bond lengths). This was done in terms of hypothetical model cluster (Fig. 2) with C_1 symmetry (for scorodite a similar cluster with 4 Fe atoms at appropriate angles was used). To use a cluster with C1 symmetry, all oxygens coordinated to As were treated independently and

constrained to have a coordination number of 1.0. Note also that the multiple scattering contributions were calculated self-consistently; that is, the bond lengths and angles (Fig. 2) were allowed to vary during the fits of the EXAFS spectra. The EXAFS fits were started with an initial ideal tetrahedral structure for the oxygen shells. The final bond angles were fairly close to those of the ideal starting geometries although the bond lengths showed some distortion.

3. RESULTS AND DISCUSSION

3.1. Predicted Geometries and Energetics of AsO_4 Surface Complexes using DFT

We calculated the optimized geometries of $Fe2(OH)_2(H_2O)_nAsO_4^{+}$ and $Fe_2(OH)_2(H_2O)_nAsO_2(OH)_2^{+3}$ clusters corresponding to ^{2}E and ^{2}C complexes of AsO_4^{3-} and $AsO_2(OH)_2^{-}$. We used a spin-unrestricted calculation and set the clusters to have a ferromagnetic configuration. The choice of a ferromagnetic vs. antiferromagnetic configuration for the $Fe_2(OH)_2(H_2O)_8$ substrate should have only a minor chemical effect. (Note that a spin-restricted calculation would be seriously in error, however, since it would mix in configurations associated with high energy multiplets as discussed by Sherman, 1985). The optimized geometries for clusters analogous to bidentate edge-sharing, corner-sharing and monodentate surface complexes are shown in Figure 3. In the ^{2}C and ^{2}E complexes (Fig. 3a,b). Note that if the AsO_4 tetrahedron is deprotonated (i.e., AsO_4^{3-}) the As-O bond lengths distort to values (~1.69 and ~1.81 Å) which are in poor agreement with experiment (discussed below). This suggests that As is sorbed as $H_2AsO_4^{-}$ at pH = 4 and 7 and not as $(AsO_4)^{3-}$; the dominant aqueous species of $H_nAsO_4^{3-n}$ over this pH range is $H_2AsO_4^{-}$.

The predicted Fe-As distances in the $Fe_2(OH)_2(H_2O)_n$ $AsO_2(OH)_2^{+3}$ cluster simulating the ^{2}C complex (Fig. 3a) is in good agreement with that found experimentally (e.g., Waychunas et al., 1995 and results obtained here). The optimized As-Fe distance in the ^{2}E complex (Fig. 3b) is somewhat shorter than that proposed by Manceau (1995) (i.e., 2.70 Å vs 2.83 Å). Most importantly, bidentate edge-sharing (^{2}E) cluster (Fig. 3b) is energetically unfavorable by 0.57 eV (55 kJ/mole) relative to the bidentate corner-sharing (^{2}C) cluster (Fig. 3a). The instability of the edge-sharing complex contradicts the proposal by Manceau (1995). This energy difference is too large to allow any significant contribution from the ^{2}E surface complex to $H_nAsO_4^{3-n}$ adsorption. For goethite, moreover, the ^{2}E complexes can only form on the {001} or {021} surfaces which comprise only a small fraction of the goethite surface (e.g., Randall et al., 1999; Boily et al., 2001).

The stoichiometry of the cluster used to model the monodentate (^{1}V) complex (Fig. 3c) differs from that of the other clusters by one water molecule. Using the same basis set and exchange-correlation functional, the static zero-point energy of a gas-phase water molecule was calculated; the energy of the reaction

$$Fe_2(OH)_2(H_2O)_7AsO_2(OH)_2^{3+}(^1V) = Fe_2(OH)_2(H_2O)_6AsO_2(OH)_2^{3+}(^2C)+H_2O \quad (1)$$

was then found to be −1.65 eV (−156 kJ/mole) for sorption of AsO_4^{-} and −0.98 eV (−95 kJ/mole) for sorption of $AsO_2(OH)_2^{-}$. This implies that the monodentate complex cannot be significant. Including the solvation of water in reaction (1) will increase energy balance in favor of the ^{2}C complex. The As-O bond in the As-O-Fe linkage of the (^{1}V) cluster is quite long (1.89 Å) and suggests that it is very weak and would be readily hydrolyzed. Note that the ^{2}C complex is also favored entropically (the chelate effect). The large energy differences between the ^{2}C, ^{1}V and ^{2}E complexes are probably exaggerated by the neglect of solvation. This might, in particular, be contributing to the predicted low stability of the ^{1}V complex. However, the solvation energies of the ^{2}C and ^{2}E complexes should be similar and we believe that the large energy difference between these complexes is real.

Ladeira et al. (2001) used analogous DFT calculations on $Al_2(OH)_6AsO_2(OH)_2$ clusters to model surface complexation of $H_2AsO_4^{-}$ on $Al(OH)_3$. They found that the bidentate corner-sharing arrangement (^{2}C) was more stable than the monodentate corner-sharing (^{1}V) and bidentate edge-sharing (^{2}E) complexes by >100 kJ/mole. Hence, their results are in reasonable quantitative agreement with ours. They used a somewhat different exchange correlation functional and basis set but also assumed that As occurs as $H_2AsO_4^{-}$.

3.2. As K-edge EXAFS Spectroscopy

3.2.1. As K-edge EXAFS of scorodite

As K-edge EXAFS (and Fourier transforms of the EXAFS) of scorodite ($FeAsO_40.4H_2O$) are given in Figure 4 and summarized in Table 1. The first coordination shell about As consists of four oxygen atoms at a distance of 1.69 Å. Aside from the tetrahedral oxygen shell, the scorodite spectra are dominated by two iron shells at As-Fe distances of 3.31 and 3.42 Å. This is in good agreement with the As-Fe distances of 3.34–3.39 Å found in the scorodite structure (Kitahama et al., 1975). Our results are also in good agreement with those of Foster et al. (1998) who also included multiple scattering in their analysis. Agreement with the known structure gives us confidence that the phase shifts (derived by ab initio calculations in EXCURV98) used during our EXAFS data analysis are accurate. The As-Fe distances in scorodite result from single corner linkages between arsenate tetrahedra and FeO_6 octahedra. Single-corner sharing with a linear As-O-Fe bond (180° bond angle) would yield an As-Fe distance near 3.65 Å. The As-Fe distance observed in scorodite is much smaller because the As-O-Fe bond angles are between 100 and 135°.

3.2.2. EXAFS of (AsO_4)-iron oxide and oxide hydroxide complexes

EXAFS and their Fourier transforms are given in Figure 5a,b for As associated with goethite, lepidocrocite, hematite and ferrihydrite. As with the scorodite EXAFS, we directly fit the EXAFS and allowed for multiple scattering based on a cluster with C_1 symmetry (Fig. 2). Each oxygen atom in the As coordination environment was treated independently. The resulting fit parameters are given in Table 1.

When AsO_4 is adsorbed to iron (hydr)oxide phases, the oxygen shell is distorted to give two oxygens at a short distance (1.62, 1.67 Å) and two at a longer distance (1.71 Å). This

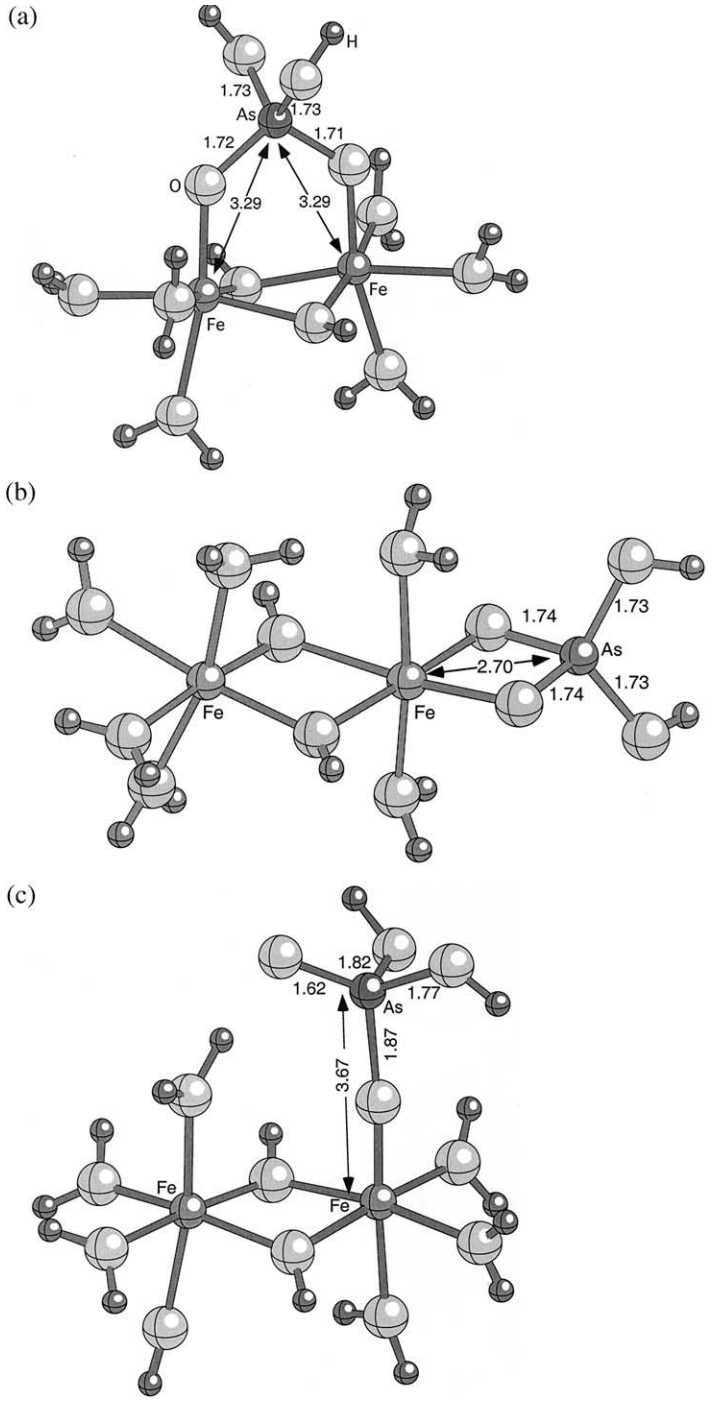

Fig. 3. Optimized geometries of $Fe_2(OH)_2(H_2O)_nAsO_4^+$ clusters calculated using density functional theory. Calculated bond lengths are given in Angstroms. The bidentate corner-sharing (^{2}C) complex (a) is more stable than the edge-sharing (^{2}E) complex (b) by 55 kJ/mole.

distortion of the AsO_4 tetrahedra was predicted for bidentate complexes in the DFT cluster simulations described above.

The phase-shift corrected Fourier transforms of the EXAFS of As sorbed to iron hydr(oxides) show peaks with apparent As-Fe distances of 2.85 Å and 3.2 – 3.35 Å. Fitting the data with a model that includes multiple scattering, however, shows that the 2.85 peak results not from As-Fe backscatter but from multiple scattering involving O-O pairs within the AsO_4 tetrahedron (Fig. 2). The significance of multiple scattering in tetrahedral oxyanions was demonstrated by Pandya (1994) for CrO_4. When multiple scattering is accounted for, it is not necessary to include an edge-sharing (^{2}E) complex in the EXAFS fits; if such a complex is included, the resulting number of Fe neighbors associated with the ^{2}E complex is small (<0.3).

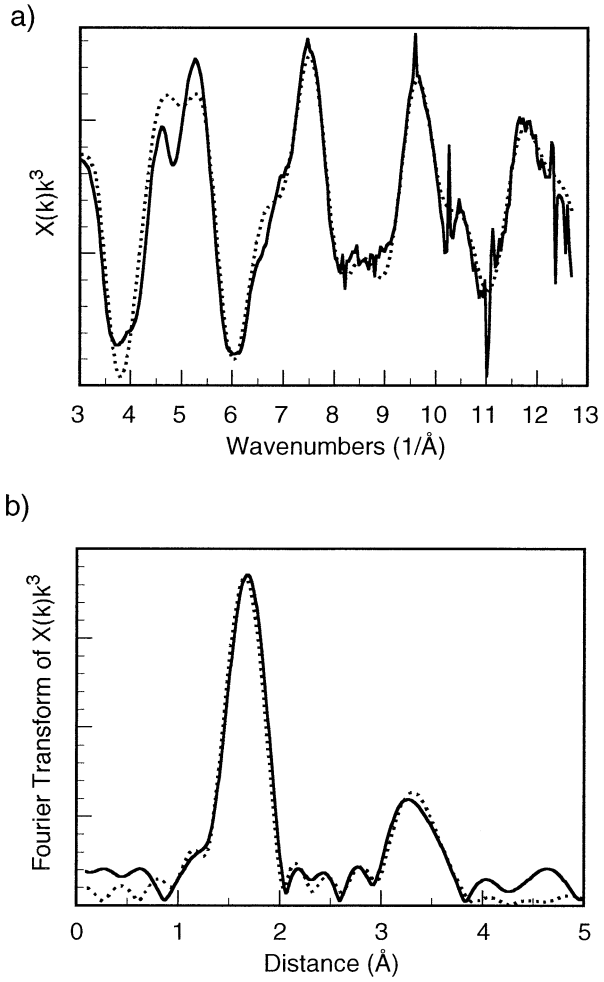

Fig. 4. a) As K-edge EXAFS spectrum and b) and the Fourier transforms of scorodite. The As-Fe distances of 3.31 – 3.41 Å in scorodite result from corner-sharing linkages.

Inclusion of the ^{2}E cluster provides no statistically significant ($\Delta R < 1\%$) improvement to the EXAFS fit. A further clue to the multiple-scattering origin of the 2.85 Å peak is the observation that the same peak is found with the same amplitude in the EXAFS of scorodite where there is no edge-sharing between FeO_6 and AsO_6 polyhedra. Also, the apparent magnitude of the 2.85 Å peak is sensitive to the lower limit chosen for the k-range. Ladeira et al. (2001) found no 2.85 peak in their EXAFS of AsO_4 on $Al(OH)_3$ because they used a k-range of 3.9–14 Å^{-1}. A Fourier transform of our data over the k-range 4–13 Å^{-1} shows no peak at 2.85 Å.

The mechanisms by which H_nAsO_4n-3 complexes to goethite, lepidocrocite, hematite and ferrihydrite appear to be identical and are identified as the bidentate corner-sharing (^{2}C) complex (Figs. 1 and 3a). This is consistent with the very large predicted energy difference between the ^{2}C and ^{2}E clusters. As pointed out by Waychunas et al. (1995) the absence of edge-sharing complexes is also consistent with the general observation that there are no known edge-sharing arrangements between $Fe^{3+}O_6$ polyhedra and tetrahedral oxyanions in crystalline solids (Kurchhof et al., 1991).

4. CONCLUSIONS

Adsorption of arsenate $H_nAsO_4^{3-n}$ onto goethite, lepidocrocite, hematite and ferrihydrite occurs by the formation of inner-sphere surface complexes resulting from bidentate corner-sharing between AsO_4 and FeO_6 polyhedra (^{2}C). The bidentate edge-sharing complexes proposed by Manceau (1995) are predicted by density functional calculations to be energetically unfavorable. Moreover, the apparent As-Fe peaks near 2.85 Å in the EXAFS spectra that have been attributed to edge-sharing complexes (Fendorf et al., 1997) can be accounted for by multiple scattering within the AsO_4 tetrahedron. Monodentate complexing (^{1}V) is also energetically unfavorable according to the cluster calculations. There is no evidence for monodentate complexes in the fits to the EXAFS spectra of As sorbed to any of the iron oxides or oxide hydroxides.

Acknowledgments—Part of this work was supported by NERC grant GR9/03506. Synchrotron time was also provided by CLRC Daresbury Laboratory. SRR's studentship was supported by BNFL. We are especially grateful to Dr. Ian Stewart, Bristol University for help in implementing software on the Beowulf cluster. We also thank Dr. D.M. Heasman and C. Muskett for help in data collection. We are grateful for the comments of two anonymous reviewers.

Table 1. Samples investigated and fits to EXAFS data. Values in italics were constrained during fitting.

Sample	As/Fe	As-O Shells N atoms at R Å ($2\sigma^2$ in Å^2)				As-Fe shells N atoms at R Å ($2\sigma^2$ in Å^2)		χ^2 (R%)
Scorodite	1.0	*1.0* at 1.62 Å (0.007)	*1.0* at 1.70 Å (0.004)	*1.0* at 1.70 Å (0.004)	*1.0* at 1.71 Å (0.004)	*2.0* at 3.31 Å (0.007)	*2.0* at 3.41 Å (0.007)	1.74 (25.)
Goethite (pH = 4.0)	0.0028	1.0 at 1.63 Å *(0.003)*	1.0 at 1.70 Å *(0.003)*	1.0 at 1.70 Å *(0.003)*	1.0 at 1.70 Å *(0.003)*	1.0 at 3.30 Å *(0.01)*	1.0 at 3.30 Å *(0.01)*	1.12 (20.)
Lepidocrocite (pH = 7.0)	0.0028	1.0 at 1.63 Å *(0.003)*	1.0 at 1.66 Å *(0.003)*	1.0 at 1.71 Å *(0.003)*	1.0 at 1.71 Å *(0.003)*	0.7 at 3.30 Å *(0.01)*	1.3 at 3.32 Å *(0.01)*	1.62 (21.)
Hematite (pH = 4.0)	0.0031	1.0 at 1.62 Å *(0.003)*	1.0 at 1.70 Å *(0.003)*	1.0 at 1.70 Å *(0.003)*	1.0 at 1.70 Å *(0.003)*	1.1 at 3.24 Å (0.01)	1.2 at 3.35 Å (0.01)	1.32 (23.)
Ferrihydrite (adsorbed at pH = 4.0)	0.0033	1.0 at 1.62 Å *(0.003)*	1.0 at 1.68 Å *(0.003)*	1.0 at 1.71 Å *(0.003)*	1.0 at 1.71 Å *(0.003)*	0.4 at 3.16 Å (0.008)	1.0 at 3.30 Å (0.009)	1.00 (20.)
Ferrihydrite (coprecipitated at pH = 4.0)	0.0054	1.0 at 1.62 Å *(0.003)*	1.0 at 1.70 Å *(0.003)*	1.0 at 1.70 Å *(0.003)*	1.0 at 1.71 Å *(0.003)*	1.3 at 3.27 Å (0.01)	1.0 at 3.38 Å (0.01)	0.89 (20.)
Ferrihydrite (adsorbed at pH = 4.0))	0.016	1.0 at 1.64 Å *(0.004)*	1.0 at 1.67 Å *(0.004)*	1.0 at 1.70 Å *(0.004)*	1.0 at 1.70 Å *(0.004)*	1.8 at 3.3 Å (0.02)		1.4 (25.)

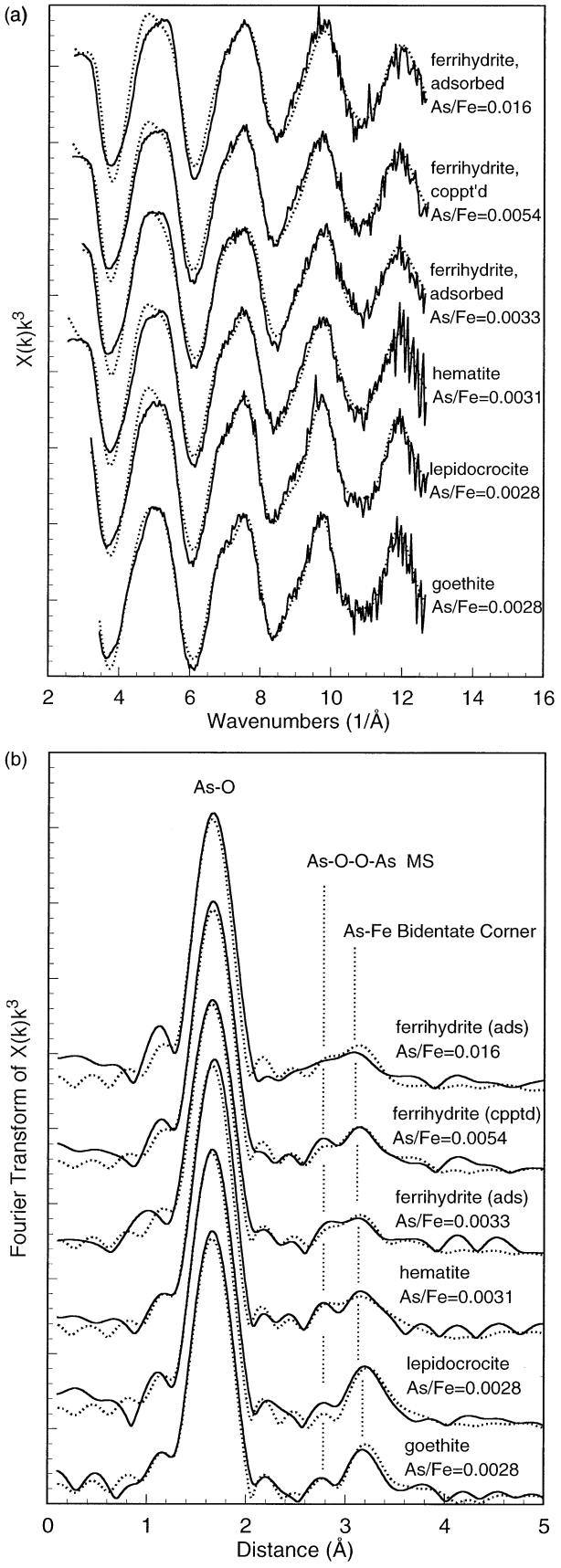

Fig. 5. a) As K-edge EXAFS spectra and b) Fourier transforms of the EXAFS for As sorbed onto goethite, lepidocrocite, hematite and ferrihydrite. The model fits that include multiple scattering are shown as dashed lines. In the Fourier transforms, the apparent peak near 2.85 results from multiple scattering; note that the same peak is also present in the scorodite RDF. The peaks near 3.3–3.4 Å results from As-Fe single-scattering and agree with the predicted distances for bindentate corner-sharing (Fig. 3a).

Associate editor: G. Helz

REFERENCES

Aggett J. and Roberts L. S. (1986) Insight into the mechanism of accumulation of arsenate and phosphate in hydro lake sediments by measuring the rate of dissolution with ethylenediamine-tetraacetic acid. *Environ. Sci. Technol.* **20**, 183–186.

Belzile N. and Tessier A. (1990) Interactions between arsenic and iron oxyhydroxides in lacustrine sediments. *Geochim. Cosmochim. Acta* **54**, 103–109.

Binsted N (1998) EXCURV98: CCLRC Daresbury Laboratory computer program. Daresbury Laboratory, Warrington, U.K.

Boily J.-F., Lutzenkirchen J., Balmes O., Beattie J., and Sjoberg S. (2001) Modeling proton binding at the goethite (α-FeOOH)-water interface. *Colloids and Surfaces A* **179**, 11–27.

Carlson L., Bigham J. M., Schwertmann U., Kyek A., and Wagner F. (2002) Scavenging of as from acid mine drainage by schwertmannite and ferrihydrite: A comparison with synthetic analogues. *Env. Sci. Technol.* **36**, 1712–1719.

Dent A. J. and Mosselmans J. F. W. (1992) *A Guide to EXBACK, EXCALIB, and EXCURV92*. Daresbury Laboratory, Warrington, U. K.

Farquhar M. L., Charnock J. M., Livens F. R., and Vaughan D. J. (2002) Mechanisms of arsenic uptake from aqueous solution by interaction with goethite, lepidocrocite, mackinawite, and pyrite: An X-ray absorption spectroscopy study. *Env. Sci. Tech.* **36**, 1757–1762.

Fendorf S., Eick M. J., Grossl P., and Sparks D. L. (1997) Arsenate and chromate retention mechanisms on goethite. 1. Surface structure. *Envrion. Sci. Technol.* **31**, 315–320.

Foster A. L., Brown G. E., Tingle T. N., and Parks G. A. (1998) Quantitative speciation of arsenic in mine tailings using X-ray absorption spectroscopy. *American Mineralogist* **89**, 553–568.

Grossl P. R. and Sparks D. L. (1995) Evaluation for contaminant ion adsorption-desorption on goethite using pressure-jump relaxation kinetics. *Geoderma* **67**, 87–101.

Grossl P. R., Eick M., Sparks D. L., Goldberg S., and Ainsworth C. C. (1997) Arsenate and chromate retention mechanisms on goethite. 2. Kinetic evaluation using a pressure-jump relaxation technique. *Envrion. Sci. Technol.* **31**, 321–326.

Gurman S. J., Binsted N., and Ross I. (1986) Multiple scattering rapid curved wave theory. *J. Phys. C: Solid State Phys* **19**, 1845–1861.

Hedin L. and Lundqvist S. (1969) Effects of electron-electron and electron-phonon interactions on the one-electron states of solids. *Solid State Phys.* **23**, 1–181.

Hsia T. H., Lo S. L., Lin C. F., and Lee D. Y. (1994) Characterization of arsenate adsorption on hydrous iron oxide using chemical and physical methods. *Colloids Surfaces A - Physicochem. Eng. Aspects* **85**, 1–7.

Jain A., Ravan K. P., and Loeppert R. H. (1999) Arsenite and arsenate adsorption on ferrihydrite: Surface charge reduction and net OH- release stoichiometry. *Env. Sci. Technol.* **33**, 1179–1184.

Kitahama K., Kiriyama R., and Baba Y. (1975) Refinement of the crystal structure of scorodite. *Acta Crysta.* **B31**, 322–324.

Kurchhof A., Pebler A., and Warkensten, eds. (1991) Inorganic crystal structure database (ICSD). Gmelin-Institute fur Anorganische Chemie.

Ladeira A. C. Q., Ciminelli V. S. T., Duarte H. A., Alves M. C. M., and Ramos A. Y. (2001) Mechanism of anion retention from EXAFS and density functional calculations: Arsenic (V) adsorbed on gibbsite. *Geochim. Cosmochim. Acta* **65**, 1211–1217.

Livesey N. T. and Huang P. M. (1981) Adsorption of arsenate by soils and its relation to selected chemical-properties and anions. *Soil Sci.* **131**, 88–94.

Manceau A. (1995) The mechanism of anion adsorption on iron oxides: Evidence for the bonding of arsenate tetrahedra on free Fe(O,OH)6 edges. *Geochim. Cosmochim. Acta* **59**, 3647–3653.

Pandya K. I. (1994) Multiple-scattering effects in x-ray absorption fine structure: Chromium in tetrahedral configuration. *Phys. Rev. B* **50**, 15509–15515.

Perdew J. P., Chevary J. A., Vosko S. H., Jackson K. A., Pederson M. R., Singh D. J., and Fiolhais C. (1992) Atoms, molecules, solids, and surfaces - applications of the generalized gradient approximation for exchange and correlation. *Phys. Rev.* **B46**, 6671–6687.

Pichler T., Veizer J., and Hall G. E. M. (1999) Natural input of arsenic into a coral reef ecosystem by hydrothermal fluids and its removal by Fe(III) oxyhydroxides. *Environmental Science and Technology* **33**, 1373–1378.

Randall S. R., Sherman D. M., Ragnarsdottir K. V., and Collins C. R. (1999) The mechanism of cadmium surface complexation on iron oxyhydroxide minerals. *Geochim. Cosmochim. Acta* **63**, 2971–2987.

Schwertmann U. and Cornell R. M. (1991) *Iron oxides in the Laboratory: Preparation and Characterization.* VCH Publishers. Weinheim.

Sherman D. M. (1985) Electronic structures of Fe^{3+} coordination sites in iron oxides: Applications to spectra, bonding and magnetism. *Phys. Chem. Mineral.* **12**, 161–175.

Sullivan K. A. and Aller R. C. (1996) Diagenetic cycling of arsenic in Amazon shelf sediments. *Geochim. Cosmochim. Acta* **60**, 1465–1477.

Sun X. H. and Doner H. E. (1996) An investigation of arsenate and arsenite bonding structures on goethite by FTIR. *Soil Science* **161**, 865–872.

te Velde G., Bickelhaupt F. M., Baerends E. J., Fonseca Guerra C., van Gisbergen S. J. A., Snijders J. G., and Ziegler T. (2001) Chemistry with ADF. *Journal of Computational Chemistry* **22**, 931–967.

Vosko S. H., Wilk K., and Nusair M. (1980) Accurate spin-dependent electron liquid correlation energy for local spin density calculations: A critical analysis. *Can. J. Phys.* **58**, 1200–1205.

Waychunas G. A., Rea B. A., Fuller C. C., and Davis J. A. (1993) Surface chemistry of ferrihydrite. 1. EXAFS studies of the geometry of coprecipitated and adsorbed arsenate. *Geochim. Cosmochim. Acta* **57**, 2251–2269.

Waychunas G. A., Davis J. A., and Fuller C. C. (1995) Geometry of sorbed arsenate on ferrihydrite and crystalline FeOOH: Re-evaluation of EXAFS results and topological factors in predicting sorbate geometry, and evidence for monodentate complexes. *Geochim. Cosmochim. Acta* **59**, 3655–3661.

Waychunas G. A., Fuller C. C., Rea B. A., and Davis J. A. (1996) Wide angle X-ray scattering (WAXS) of "two-line" ferrihydrite structure: Effect of arsenate sorption and counterion variation and comparison with EXAFS results. *Geochim. Cosmochim. Acta* **60**, 1765–1781.

Wilkie J. A. and Hering J. G. (1996) Adsorption of arsenic onto hydrous ferric oxide - effects of adsorbate/adsorbent ratios and co-occurring solute. *Colloids and Surfaces A - Physicochem. Eng. Aspects* **107**, 97–110.